Journal of Superconductivity: Incorporating Novel Magnetism, Vol. 16, No. 5, October 2003 (© 2003)

Deposition and Properties of Superconducting MgB_2 Thin Films

X. X. Xi,[1] X. H. Zeng,[1] A. V. Pogrebnyakov,[1] A. Soukiassian,[1] S. Y. Xu,[1] Y. F. Hu,[1] E. Wertz,[1] Q. Li,[1] Y. Zhong,[2] C. O. Brubaker,[2] Z.-K. Liu,[2] E. M. Lysczek,[2] J. M. Redwing,[2] J. Lettieri,[2] D. G. Schlom,[2] W. Tian,[3] H. P. Sun,[3] and X. Q. Pan[3]

Received September 30, 2002

The recently discovered superconductor MgB_2 with T_c at 39 K has great potential in superconducting electronics. In this paper, we review the deposition techniques used for MgB_2 thin films in the light of a thermodynamic study of the Mg-B system with the calculation of phase diagrams (CALPHAD) modeling technique. This thermodynamic study identifies a growth window in the pressure–temperature phase diagram, in which the magnesium pressure is very high for likely *in situ* growth temperatures. A Hybrid Physical–Chemical Vapor Deposition (HPCVD) technique that successfully achieves such a high Mg pressure is shown to produce *in situ* epitaxial MgB_2 thin films with bulk superconducting properties.

KEY WORDS: MgB_2; thin films; deposition techniques.

1. INTRODUCTION

The 39-K superconductor magnesium diboride [1] is very attractive for superconducting electronics. Compared to high-temperature superconductors (HTS), MgB_2 is a BCS superconductor [2] with longer coherence length [3] and smaller anisotropy [4]. The grain boundaries are not weak links [5,6]. One should thus be able to make MgB_2 Josephson junctions much more easily and reproducibly as compared to HTS. Even for microwave devices, the lack of weak link in MgB_2 may lead to much better power handling capability than HTS, thus enabling active microwave device applications. Compared to low-T_c superconductors, i.e., Nb, MgB_2 has a much higher T_c and larger energy gap (even with two gaps [7,8]), which potentially means higher speeds. Increasing the operation temperature from 5 K for Nb to 20 K for MgB_2 is a "big deal." A MgB_2 technology with high speed and 20 K operation, using a much cheaper and much more reliable cryocooler than those necessary for 5 K operation, will make superconducting electronics much more competitive.

High quality thin films are necessary for superconducting electronics using MgB_2. However, because of the high volatility of Mg the fabrication of MgB_2 thin films is difficult. In this paper, we discuss a thermodynamic analysis of the Mg-B system, which shows that the MgB_2 phase is thermodynamically stable only under high Mg partial pressures. The result provides helpful insights into appropriate processing conditions for *in situ* deposition of MgB_2 thin films as well as the limitations of the deposition techniques involving postdeposition annealing. Finally, we show that epitaxial MgB_2 thin films can be deposited *in situ* by HPCVD, a novel combination of Physical Vapor Deposition (PVD) and Chemical Vapor Deposition (CVD) [9].

2. THERMODYNAMICS OF THE Mg-B SYSTEM

Our approach of the thermodynamic analysis is the calculation of phase diagrams (CALPHAD)

[1]Department of Physics, The Pennsylvania State University, University Park, Pennsylvania 16802.
[2]Department of Materials Science and Engineering, The Pennsylvania State University, University Park, Pennsylvania 16802.
[3]Department of Materials Science and Engineering, The University of Michigan, Ann Arbor, Michigan 48109.

0896-1107/03/1000-0801/0 © 2003 Plenum Publishing Corporation

thermodynamic modeling technique using a computerized optimization procedure [10]. The Gibbs energies of formation for individual phases in the Mg-B system, i.e. MgB_2, MgB_4, and MgB_7 in addition to gas, liquid, *hcp* magnesium, and β-rhombohedral boron, are constructed. Using the experimentally measured enthalpy of formation and estimated decomposition temperatures, the Gibbs energy of each phase is evaluated with the ThermoCalc program [11]. The phase equilibria are then calculated.

The pressure–temperature phase diagram for all compositions with $x_{Mg}/x_B \geq 1{:}2$ is shown in Fig. 1 [12]. From a thermodynamic perspective, deposition of a single-phase MgB_2 film becomes easy when the growth conditions (substrate temperature and Mg pressure) fall within a window where the thermodynamically stable phases are the desired MgB_2 phase and gas phases, which is marked by "Gas + MgB_2" in Fig. 1. The boundaries of the growth window can be approximately expressed by the following equations: $\log(P) = -7561/T + 8.673$ (the upper boundary with solid Mg), and $\log(P) = -10142/T + 8.562$ (the lower boundary with MgB_4), where P is in Torr and T in Kelvin. An inspection of the phase diagram reveals that the growth window for MgB_2 is located at very high Mg partial pressures. For a deposition temperature, for example, of 750°C, a Mg pressure greater than 44 mTorr is necessary to keep the MgB_2 phase thermodynamically stable. This is very high for many vacuum deposition techniques, and it clearly favors deposition techniques that can maintain a high Mg pressure during the deposition. This is further complicated by the oxygen contamination during the deposition. The Mg flux reacts with residual oxygen in the background, which effectively reduces the Mg pressure thus pushing the system to the thermodynamically unstable region.

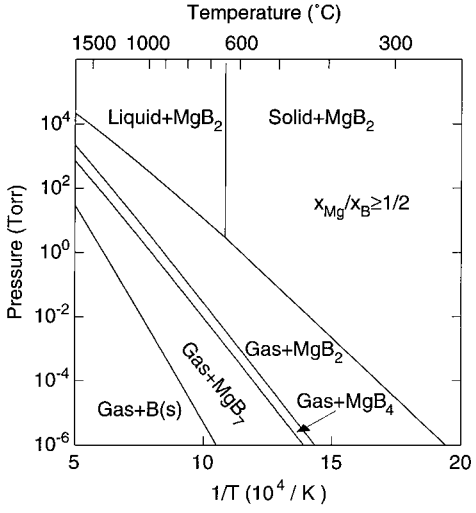

Fig. 1. The pressure-temperature phase diagram for the Mg-B system (Mg:B atomic ratio $x_{Mg}/x_B \geq 1/2$) [12]. The region of "Gas + MgB_2" represent the thermodynamic stability window for the deposition of MgB_2 thin films.

While the applicability of equilibrium thermodynamics to thin film growth has been established for many material systems [13–16], the nonequilibrium nature of specific deposition techniques can be quite important. For MgB_2, Fan *et al.* has shown that a significant kinetic barrier to the thermal decomposition of MgB_2 exists [17]. Once the formation reaction of MgB_2 phase is achieved, MgB_2 may not decompose even at a Mg pressure as much as a factor of 10^{-3} lower than that predicted in the phase diagram in Fig. 1. In this paper, the analysis of various techniques is made mainly on the equilibrium thermodynamic considerations.

3. MgB_2 FILMS GROWN BY TECHNIQUES REQUIRING ANNEALING

3.1. *Ex Situ* Annealing in Mg Vapor

Epitaxial thin films requires sufficiently high-growth temperatures, typically about one half of the melting temperature T_m (in Kelvin). MgB_2 melts congruently at 2430°C (~2700 K) under 49,000 Torr pressure, thus the optimum temperature for epitaxial MgB_2 films is around ~1080°C (1350 K). This requires a Mg pressure of at least 11 Torr, impossible for many thin film deposition techniques. However, it can easily generated by heating Mg bulk in an enclosure, which is the thermodynamic basis for growth of MgB_2 thin films with *ex situ* annealing in Mg vapor.

In one report of such technique [18], Kang *et al.* first deposited amorphous B thin films at room temperature by pulsed laser deposition. The precursor thin film was then put into a Ta tube together with a high-purity Mg metal and sealed in an Ar atmosphere. The sample was quickly heated to 900°C in 5 min, held at this temperature for 10–30 min, and then quenched to room temperature. Besides pulsed laser deposition [19–21], the pure B films have been deposited by RF magnetron sputtering [22], electron-beam evaporation [23,24], and thermal evaporation [25]. The annealing temperatures used range from 750–950°C [21]. Alternatively, the precursor films can

also be deposited from a MgB_2 target [26]. Similar procedure has even been reported on B crystals [27].

It has been reported that the MgB_2 thin films grown by *ex situ* annealing in Mg vapor are epitaxial [21,22]. In a MgB_2 film on c-plane sapphire substrate annealed at 950°C, Berenov *et al*. showed strong in-plane biaxial alignment between the film and substrate evidenced by a sixfold symmetry in the ϕ-scan of the X-ray diffraction [21]. The hexagonal lattice of MgB_2 is rotated by 30° to match that of Al_2O_3. The epitaxy with the same in-plane alignment is clearly shown by Bu *et al*. by both X-ray diffraction and cross-sectional TEM in sputtered B films annealed at 850°C [22].

The superconducting properties of the MgB_2 thin films grown by *ex situ* annealing in Mg vapor are bulk-like. They show T_c ~39 K [18,19,23,24] and very high J_c exceeding 10^7 A/cm^2 at zero field [24,28]. Unfortunately, the surface of these films is rough [20,29]. The surface is likely covered by a Mg-rich layer, which results in high microwave surface resistance [30,31]. Removal of this layer leads to significant reduction of the surface resistance [30]. Planar Josephson junctions have been made on such films by milling a trench with a depth of 70 and 80% of the film thickness [32]. Multilayer $Nb/Al_2O_3/Al/MgB_2$ junctions have also been reported where a 10-nm surface layer of the MgB_2 film was removed before further junction precessing [33].

3.2. *In Situ* Annealing of Films With Excess Mg

As the high-temperature *ex situ* annealing is not desirable for multilayer device fabrication, an alternative type of techniques have been used that employ *in situ* annealing in the growth chamber at temperatures and duration such that severe Mg loss or MgB_2 decomposition does not occur [19,25,34–36, N. Newman, private communication, 2002]. The films are deposited at low temperatures ranging from room temperature to 300°C. The deposition techniques include pulsed laser deposition [19,34–36,37], sputtering [38], or thermal evaporation [25,N. Newman, private communication, 2002]. The films are deposited from sources of either MgB_2, $Mg+MgB_2$, or Mg+B. In some cases, multilayer structures are used [19,35].

Several processes are involved in the *in situ* annealing: Mg evaporation, MgB_2 phase formation, nucleation and growth of crystallites, and MgB_2 decomposition. These processes are determined by the thermodynamics [12] and kinetics [17], and a balance among these processes by carefully adjusting the heating and annealing parameters is critical. As the annealing is carried out in either vacuum [37] or Ar atmosphere [34–36,38], the Mg pressure is provided locally by the evaporation of excess Mg in the films. Since the Mg supply is limited, the local Mg pressure changes with time during the annealing and eventually drops. Therefore, if the annealing temperature is too high and/or the annealing time is too long, the low Mg pressure will result in the decomposition of MgB_2. Here, the kinetic barrier for MgB_2 decomposition plays a particularly important role [17]. Several successful annealing procedures include: 600–650°C for less than 10 min [34–36,37,38], and up to 900°C for a very short time [25,N. Newman, private communication, 2002].

Films produced by the *in situ* annealing techniques are polycrystalline [36]. It is common that the X-ray or electron diffraction signals from MgB_2 in these films are very weak due to the small grain size [35,36,37,38]. In Fig. 2, a θ-2θ scan of X-ray diffraction using synchrotron radiation is shown for a MgB_2 film grown with *in situ* annealing in our lab. With the help of the high X-ray intensity of the synchrotron source, we are able to observe the weak (002) diffraction peak because of MgB_2. From the width of the peak, the grain size of MgB_2 is estimated to be between 50–70 Å, consistent with our estimation from the cross-section TEM [36].

The T_c of *in situ* annealed MgB_2 films from the early reports was around or below 25 K [19,34,35,39]. More recent result shows higher T_c at (34 K) [36,N. Newman, private communication, 2002]. This demonstrates the difficulty in obtaining a perfect balance among the various processes during the annealing.

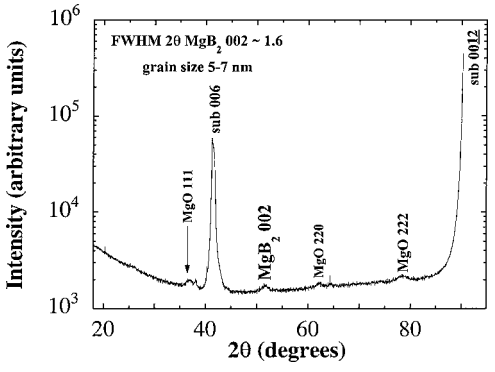

Fig. 2. X-ray diffraction θ-2θ scan of a MgB_2 film on a (0001) sapphire substrate deposited by pulsed laser deposition with *in situ* annealing.

The J_c is reported to be over 10^6 A/cm^2 at low temperatures [36]. The surface of these films are smoother than the *ex situ* annealed films [29,40]. The microwave surface resistance of such films directly reveal an exponential behavior with a value of $10^{-5}\Omega$ at low temperatures, indicating a fully gapped order parameter with $\Delta(0) = 1.9$ meV [40]. Both nanobridge [41] and ramp-type [42] junctions have been reported on *in situ* annealed films.

4. MgB_2 FILMS BY *IN SITU* GROWTH

4.1. Low-Temperature *In Situ* Growth

Although epitaxial growth prefers sufficiently high temperatures, the minimum growth temperature can be much lower. This will greatly reduce the Mg pressure requirement. For example, at a deposition temperature of 300°C, the Mg pressure of the MgB_2 growth window is from 10^{-8}–10^{-4} Torr, easily achievable by vacuum deposition techniques. However, two other factors place additional constraint: oxygen contamination and sticking coefficient of Mg. Oxygen from either the background atmosphere or the target/source react with Mg to form MgO, which not only effectively reduces the Mg pressure, but also prevents the grain growth of MgB_2. (Eom *et al*. have suggested that the oxygen contamination may help to enhance the flux pinning in MgB_2 films [26].) The sticking coefficient of Mg, on the other hand, decreases dramatically when the substrate temperature increases above 300°C [N. Newman, private communication, 2002,43]. If there is not enough Mg at the substrate to react with B, MgB_2 cannot be formed. These could explain the limited success in some low-temperature *in situ* growth of MgB_2 [40,44].

The more successful low-temperature *in situ* growth of MgB_2 thin films was first reported by Ueda and Naito [43]. They prepared the MgB_2 films by molecular beam epitaxy with a base pressure of 12×10^{-9} Torr from pure metal sources using multiple electron-beam evaporators. As-grown superconducting MgB_2 thin films were obtained when the substrate temperature was between 150–320°C with the best $T_c \sim 36$ K for 320°C. Similar technique was used by Jo *et al.*, who reported a T_c of 35 K [45]. The films by Jo *et al*. showed very clear MgB_2 peaks in the X-ray diffraction and the grains are as large as 400 Å. These results are very encouraging since the low-temperature process could be better compatible to the existing technologies for low T_c superconducting electronics.

The success of Ueda and Naito and Jo *et al*. is most likely due to the low oxygen contamination. This results partly from the UHV background in the deposition systems, and partly from the pure metal sources which contain minimal oxygen. The reason that they were not able to go to higher temperatures for better crystallization is either the sharply decreasing Mg-sticking coefficient or the remaining oxygen which reduces the Mg pressure.

4.2. *In Situ* Growth of Epitaxial MgB_2 Films

To generate a high Mg vapor pressure for *in situ* growth of MgB_2 thin films, a high-pressure process such as CVD is preferred. In the HPCVD technique we have developed, the total pressure during the deposition is 100–700 Torr. We use hydrogen as the carrier gas and use diborane (B_2H_6) as the boron precursor gas. Unlike conventional CVD which utilizes gaseous sources only, we use heated bulk Mg (99.95%) as the Mg source. The bulk pieces of Mg are placed near the substrate and are heated together with the substrate to 730–760°C. A high Mg pressure is thus generated locally around the substrate.

Once the necessary high-Mg pressure for the MgB_2-growth temperature is generated, the HPCVD process works beautifully [9]. The MgB_2 films grow epitaxially on (0001) sapphire and (0001) 4H-SiC substrates. Figure 3 shows the θ–2θ and ϕ scans of a MgB_2 film on a (0001) sapphire substrate. The c axis of the film is normal to the substrate surface, and the sixfold symmetry in Fig. 3(b) indicates an in-plane epitaxy. The hexagonal MgB_2 lattice is rotated by 30° to match the hexagonal lattice of sapphire. The small peaks at $30° \pm n\ 60°$ (where n is an integer) indicates minimal amounts of 30° rotational twinning.

The epitaxial MgB_2 films show a bulk-like T_c of 39 K, a J_c(4.2 K) of 1.2×10^7 A/cm^2 in zero field, and a $H_{c2}(0)$ of 29.2 T in parallel magnetic field. The J_c drops under applied magnetic fields faster than in *ex situ* annealed films with substantial oxygen contamination [26]. This is likely due to the minimal oxygen contamination in the films as shown by the X-ray diffraction and cross-section TEM [9]. We attribute this to the reducing hydrogen ambient in the process. The surface of the *in situ* epitaxial film is smooth with a root-mean-square roughness of 2.5 nm for MgB_2 films on SiC.

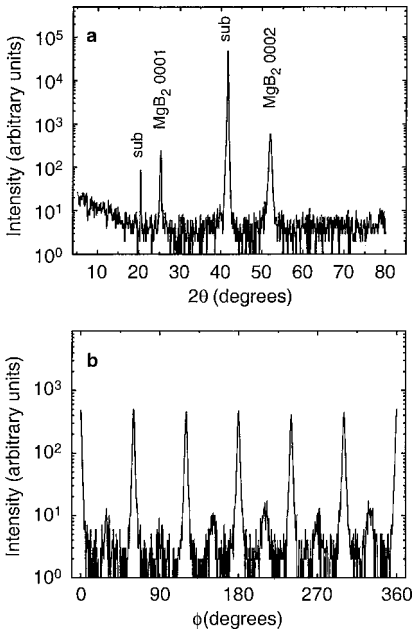

Fig. 3. X-ray diffraction spectra of a MgB_2 film on a (0001) sapphire substrate deposited *in situ* by HPCVD [9].(a) The θ-2θ scan. (b) The ϕ scan.

The excellent epitaxy and superconducting properties of the MgB_2 films by HPCVD demonstrate that *in situ* growth of high-quality epitaxial MgB_2 films is possible as long as a sufficiently high Mg vapor pressure is produced. At the growth temperature of $\sim$750°C, the HPCVD successfully achieves a pressure of about 44 mTorr according to the thermodynamic growth window [12]. The low sticking coefficient of Mg at this high temperature help to make the process simple. When the B_2H_6 gas is not flowing through the reactor, there is no film deposition because of the low sticking coefficient of Mg [N. Newman, private communication, 2002]. Once the B_2H_6 gas begins to flow, a MgB_2 film starts to grow on the substrate. After the growth when the B_2H_6 gas is switched off, again Mg does not stick, leaving a clean MgB_2 film surface.

5. CONCLUSION

The thermodynamic analysis has provided a general guidance towards a successful deposition technique for *in situ* epitaxial MgB_2 thin films. Because thin film deposition is not exactly a phase equilibrium problem, deviations from the thermodynamic phase diagram should be expected. For example, decomposition kinetics and sticking coefficient have been shown to be important. The central prediction of the thermodynamics is a growth window in the pressure-temperature phase diagram, in which the Mg pressure is very high for MgB_2. It is difficult for vacuum deposition techniques to achieve at high temperatures. Reaction of Mg with oxygen during the deposition further reduces the Mg pressure. In practice, annealing B films *ex situ* in high Mg vapor pressure allows high annealing temperatures. The *in situ* growth of MgB_2 thin films has been demonstrated at low temperatures where the necessary Mg vapor pressure for phase stability is low. The *in situ* annealing technique requires a careful control of annealing temperature and duration as the local Mg pressure changes with time. The high pressure process of HPCVD successfully achieves the high Mg pressure, thus results in very high quality *in situ* epitaxial MgB_2 thin films.

ACKNOWLEDGMENTS

We thank Yufei Hu for the X-ray diffraction at the National Synchrotron Light Source at Brookhaven National Laboratory. This work is supported in part by ONR under Grant No. N00014-00-1-0294 (XXX) and N0014-01-1-0006 (JMR), by NSF under grant No. DMR-9875405 and DMR-9871177 (XQP), DMR-9876266 and DMR-9972973 (QL), DMR-9983532 (ZKL), and by DOE through grant DE-FG02-97ER45638 (DGS).

REFERENCES

1. J. Nagamatsu, N. Nakagawa, T. Muranaka, Y. Zenitani, and J. Akimitsu, *Nature* **410,** 63 (2001).
2. S. L. Bud'ko, G. Lapertot, C. Petrovic, C. E. Cunningham, N. Anderson, and P. C. Canfield, *Phys. Rev. Lett.* **86,** 1877 (2001).
3. D. K. Finnemore, J. E. Ostenson, S. L. Bud'ko, G. Lapertot, and P. C. Canfield, *Phys. Rev. Lett.* **86,** 2420 (2001).
4. M. H. Jung, M. Jaime, A. H. Lacerda, G. S. Boebinger, W. N. Kang, H. J. Kim, E. M. Choi, and S. I. Lee, *Chem. Phys. Lett.* **343,** 447 (2001).
5. D. C. Larbalestier, L. D. Cooley, M. O. Rikel, A. A. Polyanskii, J. Jiang, S. Patnaik, X. Y. Cai, D. M. Feldmann, A. Gurevich, A. A. Squitieri, *et al.*, *Nature* **410,** 186 (2001).
6. Y. Bugoslavsky, G. K. Perkins, X. Qi, L. F. Cohen, and A. D. Caplin, *Nature* **410,** 563 (2001).
7. S. Tsuda, T. Yokoya, T. Kiss, Y. Takano, K. Togano, H. Kito, H. Ihara, and S. Shin, *Phys. Rev. Lett.* **87,** 177006 (2001).
8. H. Schmidt, J. F. Zasadzinski, K. E. Gray, and D. G. Hinks, *Phys. Rev. Lett.* **88,** 127002 (2002).
9. X. H. Zeng, A. V. Pogrebnyakov, A. Kotcharov, J. E. Jones, X. X. Xi, E. M. Lysczek, J. M. Redwing, S. Y. Xu, Q. Li, J. Lettieri, *et al.*, *Nat. Mater.* **1,** 35 (2002).

10. Z.-K. Liu, Y. Zhong, D. Schlom, X. X. Xi, and Q. Li, *CALPHAD* **25,** 299 (2001).
11. B. Jansson, B. Jonsson, B. Sundman, and J. Agren, *Thermochim. Acta* **214,** 93 (1993).
12. Z. K. Liu, D. G. Schlom, Q. Li, and X. X. Xi, *Appl. Phys. Lett.* **78,** 3678 (2001).
13. R. Heckingbottom, G. Davies, and K. Prior, *Surf. Sci.* **132,** 375 (1983).
14. H. Seki and A. Koukitu, *J. Cryst. Growth* **78,** 342 (1986).
15. R. H. Hammond and R. Bormann, *Physica C* **162,** 703 (1989).
16. C. D. Theis, J. Yeh, D. G. Schlom, M. E. Hawley, and G. W. Brown, *Thin Solid Films* **325,** 107 (1998).
17. Z. Y. Fan, D. G. Hinks, N. Newman, and J. M. Rowell, *Appl. Phys. Lett.* **79,** 87 (2001).
18. W. N. Kang, H.-J. Kim, E.-M. Choi, C. U. Jung, and S.-I. Lee, *Science* **292,** 1521 (2001).
19. S. R. Shinde, S. B. Ogale, R. L. Greene, T. Venkatesan, P. C. Canfield, S. Bud'ko, G. Lapertot, and C. Petrovic, *Appl. Phys. Lett.* **79,** 227 (2001).
20. C. Ferdeghini, V. Ferrando, G. Grassano, W. Ramadan, E. Bellingeri, V. Braccini, D. Marré, P. Manfrinetti, A. Palenzona, F. Borgatti, *et al*., *Supercond. Sci. Technol*. **14,** 952 (2001).
21. A. Berenov, Z. Lockman, X. Qi, J. L. MacManus-Driscoll, Y. Bugoslavsky, L. F. Cohen, M.-H. Jo, N. A. Stelmashenko, V. N. Tsaneva, M. Kambara, *et al*., *Appl. Phys. Lett.* **79,** 4001 (2001).
22. S. D. Bu, D. M. Kim, J. H. Choi, J. Giencke, S. Patnaik, L. Cooley, E. E. Hellstrom, D. C. Larbalestier, C. B. Eom, J. Lettieri, *et al*., *Appl. Phys. Lett.* **81,** 1851 (2002).
23. M. Paranthaman, C. Cantoni, H. Y. Zhai, H. M. Christen, T. Aytug, S. Sathyamurthy, E. D. Specht, J. R. Thompson, D. H. Lowndes, H. R. Kerchner, *et al*., *Appl. Phys. Lett.* **78,** 3669 (2001).
24. S. H. Moon, J. H. Yun, H. N. Lee, J. I. Kye, H. G. Kim, W. Chung, and B. Oh, *Appl. Phys. Lett.* **79,** 2429 (2001).
25. A. Plecenik, L. Satrapinsky, P. Kúš, Š. Gaži, Š. Beňačka, I. Vávra, and I. Kostič, *Physica C* **363,** 224 (2001).
26. C. B. Eom, M. K. Lee, J. H. Choi, L. Belenky, X. Song, L. D. Cooley, M. T. Naus, S. Patnaik, J. Jiang, M. O. Rikel, *et al*., *Nature* **411,** 558 (2001).
27. N. Hur, P. A. Sharma, S. Guha, M. Z. Cieplak, D. J. Werder, Y. Horibe, C. H. Chen, and S.-W. Cheong, *Appl. Phys. Lett.* **79,** 4180 (2001).
28. H.-J. Kim, W. N. Kang, E.-M. Choi, M.-S. Kim, K. H. P. Kim, and S.-I. Lee, *Phys. Rev. Lett.* **87,** 087002 (2001).
29. H. Y. Zhai, H. M. Christen, L. Zhang, M. Paranthaman, C. Cantoni, B. C. Sales, P. H. Fleming, D. K. Christen, and D. H. Lowndes, *J. Mater. Res.* **16,** 2759 (2001).
30. S. Y. Lee, J. H. Lee, J. H. Lee, J. S. Ryu, J. Lim, S. H. Moon, H. N. Lee, H. G. Kim, and B. Oh, *Appl. Phys. Lett.* **79,** 3299 (2002).
31. A. A. Zhukov, A. Purnell, Y. Miyoshi, Y. Bugoslavsky, Z. Lockman, A. Berenov, H. Y. Zhai, H. M. Christen, M. P. Paranthaman, D. H. Lowndes, *et al*., *Appl. Phys. Lett.* **80,** 2347 (2002).
32. G. Burnell, D.-J. Kang, H. N. Lee, S. H. Moon, B. Oh, and M. G. Blamire, *Appl. Phys. Lett.* **79,** 3464 (2001).
33. G. Carapella, N. Martucciello, G. Costabile, C. Ferdeghini, V. Ferrando, and G. Grassano, *Appl. Phys. Lett.* **80,** 2949 (2002).
34. D. H. A. Blank, H. Hilgenkamp, A. Brinkman, D. Mijatovic, G. Rijnders, and H. Rogalla, *Appl. Phys. Lett.* **79,** 394 (2001).
35. H. Christen, H. Zhai, C. Cantoni, M. Paranthaman, B. Sales, C. Rouleau, D. Norton, D. Christen, and D. Lowndes, *Physica C* **353,** 157 (2001).
36. X. H. Zeng, A. Sukiasyan, X. X. Xi, Y. F. Hu, E. Wertz, Q. Li, W. Tian, H. P. Sun, X. Q. Pan, J. Lettieri, *et al*., *Appl. Phys. Lett.* **79,** 1840 (2001).
37. H. Y. Zhai, H. M. Christen, L. Zhang, C. Cantoni, M. Paranthaman, B. C. Sales, D. K. Christen, and D. H. Lowndes, *Appl. Phys. Lett.* **79,** 2603 (2001).
38. S. N. Ermolov, M. V. Indenbom, A. N. Rossolenko, I. K. Bdikin, L. S. Uspenskaya, N. S. Stepakov, and V. G. Glebovskii, *JETP Lett.* **73,** 557 (2001).
39. G. Grassano, W. Ramadan, V. Ferrando, E. Bellingeri, D. Marré, C. Ferdeghini, G. Grasso, M. Putti, A. S. Siri, P. Manfrinetti, *et al*., *Supercond. Sci. Techno.* **14,** 762 (2001).
40. N. Hakim, C. Kusko, S. Sridhar, A. Soukiassian, X. H. Zeng, and X. X. Xi, *Appl. Phys. Lett.* (2002), Manuscript submitted for publication.
41. A. Brinkman, D. Veldhuis, D. Mijatovic, G. Rijnders, D. H. A. Blank, H. Hilgenkamp, and H. Rogalla, *Appl. Phys. Lett.* **79,** 2420 (2001).
42. D. Mijatovic, A. Brinkman, I. Oomen, G. Rijnders, H. Hilgenkamp, H. Rogalla, and D. Blank, *Appl. Phys. Lett.* **80,** 2141 (2002).
43. K. Ueda and M. Naito, *Appl. Phys. Lett.* **79,** 2046 (2001).
44. A. Saito, A. Kawakami, H. Shimakage, and Z. Wang, *Jpn. J. Appl. Phys.* **41,** L127 (2002).
45. W. Jo, J.-Huh, T. Ohnishi, A. F. Marshall, M. R. Beasley, and R. H. Hammond, *Appl. Phys. Lett.* **80,** 3563 (2002).